

Characterization of naturally Epstein–Barr virus-infected gastric carcinoma cell line YCCEL1

Do Nyun Kim,¹ Min Koo Seo,¹ Hoyun Choi,¹ Su Yeon Kim,¹ Hee Jong Shin,¹ A-Ran Yoon,¹ Qian Tao,² Sun Young Rha^{3†} and Suk Kyeong Lee^{1†}

Correspondence
Suk Kyeong Lee
sukklee@catholic.ac.kr
Sun Young Rha
rha7655@yuhs.ac

¹Department of Medical Lifescience, Research Institute of Immunobiology, College of Medicine, Catholic University of Korea, Seoul, Republic of Korea

²Department of Clinical Oncology, Chinese University of Hong Kong and CUHK Shenzhen Research Institute, Hong Kong, PR China

³Department of Internal Medicine, Yonsei University College of Medicine, Seoul, Republic of Korea

Epstein–Barr virus (EBV) is a herpesvirus associated with lymphomas and carcinomas. While EBV-associated epithelial cell lines are good model systems to investigate the role of EBV in carcinoma, only a few cell lines are available as they are hard to acquire. A greater variety of naturally EBV-infected cell lines which are derived from tumour patients are needed to represent various features of EBVaGC. We characterized cell line YCCEL1, established from a Korean EBVaGC patient, to ascertain whether it can be used to study the roles of EBV in EBVaGC. The expression of EBV genes and cell surface markers was examined by *in situ* hybridization, RT-PCR, Western blot analysis, immunofluorescence assay and Northern blot analysis. EBV episomal status was analysed by Southern blotting and real-time PCR. This cell line expressed EBV nuclear antigen 1 (EBNA1) and latent membrane protein 2A (LMP2A), but not EBNA2, LMP2B nor LMP1. The majority of the lytic proteins were not detected in YCCEL1 cells either before or after treatment with 12-*O*-tetradecanoylphorbol-13-acetate. YCCEL1 cells expressed BART microRNAs (miRNAs) at high level but did not express BHRF1 miRNAs. YCCEL1 cells expressed cytokeratin, but not CD21 and CD19, suggesting CD21-independent EBV infection. The latent EBV gene and EBV miRNA expression pattern of YCCEL1 cells closely resembled that of general EBVaGC cases. Our results support the value of YCCEL1 cells as a good model system to study the role of EBV in gastric carcinogenesis.

Received 13 June 2012

Accepted 19 November 2012

INTRODUCTION

Epstein–Barr virus (EBV) is a herpesvirus that infects more than 90 % of the world's adult population. EBV is associated with Burkitt's lymphoma (BL), Hodgkin's disease, gastric carcinoma (GC), nasopharyngeal carcinoma (NPC), NK/T cell lymphoma and post-transplant lymphoproliferative disorder (Middeldorp *et al.*, 2003; Miller & Lipman, 1973; Miller *et al.*, 1969). Approximately, 10 % of global GC cases are EBV-associated (Middeldorp *et al.*, 2003; Takada, 2000). Infection of B lymphocytes by EBV is mediated by the interaction of viral glycoprotein gp350 with EBV receptor CD21 expressed on the surface of B-cells (Nemerow *et al.*, 1987). The mechanism of EBV infection for epithelial cells that lack CD21 expression is unclear (Young & Rickinson, 2004).

EBV-associated carcinoma cell lines would serve as good model systems to study the role of EBV in carcinoma.

However, EBV-infected epithelial cell lines are hard to acquire as, *in vitro*, EBV infection of epithelial cells is more complex than that of B-cells (Shannon-Lowe *et al.*, 2006; Takada, 2000). Furthermore, EBV-infected NPC cells tend to lose the EBV genome during passages *in vitro* (Danve *et al.*, 2001; Teramoto *et al.*, 2000).

EBV-positive GC cell lines reported so far include KT (Iwasaki *et al.*, 1998), GT38, GT39 (Takasaka *et al.*, 1998), AGS-EBV-GFP (Tajima *et al.*, 1998) and SNU-719 (Oh *et al.*, 2004; Park *et al.*, 1997). KT is a transplantable human EBV-associated GC (EBVaGC) that can be continuously passaged through severe combined immunodeficient (SCID) mice (Iwasaki *et al.*, 1998). It is useful to study the role of EBV in a whole body system, but the cells cannot be cultured, hindering *in vitro* experiments. GT38 and GT39 are derived from the normal tissues of EBVaGC patients. These cells show latency III as they express EBV nuclear antigen 1 (EBNA1), EBNA2, latent membrane protein 1 (LMP1), Z EBV replication activator (ZEBRA=Zta=BZLF1) and early

†These authors contributed equally to this work/paper.

antigen-diffuse (EA-D). Thus, the latency type of GT38 and GT39 cells differs from that of most EBVaGC, which show modified latency I with EBNA1 and LMP2A expression (Takasaka *et al.*, 1998).

AGS-EBV-GFP is a GC cell line infected with a recombinant EBV, which displays similar latency to that of general EBVaGC (Yoshiyama *et al.*, 1997). AGS-EBV-GFP is a valuable model system as it can be paired with AGS to clarify the role of EBV infection in GC (Shimizu *et al.*, 1996; Yoshiyama *et al.*, 1995). One caveat is that this cell line is established by artificially infecting an EBV-negative AGS GC cell line with a recombinant EBV originated from a BL cell line.

SNU-719 is established from EBVaGC tissue and expresses EBNA1 and LMP2A, but not LMP1 and EBNA2, showing similar latency to general EBVaGC; it can serve as a good model for EBVaGC (Oh *et al.*, 2004). More diverse EBV-infected GC cell lines naturally infected with EBV, such as SNU-719, are needed for research concerning the various features of EBVaGC.

In this study, we report the identification and characterization of YCCEL1, a GC cell line established from a Korean EBVaGC patient through natural infection by EBV. The YCCEL1 cell line could serve as a useful model for EBVaGC research.

RESULTS

Detecting EBV in YCCEL1

To confirm the infection of EBV at a single-cell level, YCCEL1 cells were analysed by *in situ* hybridization for EBV encoded RNA (EBER) expression. Staining of EBER in the nuclei of the EBV-positive B95-8 cells and YCCEL1 cells confirmed the presence of EBERs, while EBV-negative BJAB cells did not show any staining (Fig. 1a). PCR was carried out with unique primers that could detect PCR products of different sizes for EBNA2, EBNA3A and EBNA3C to distinguish two different EBV types: types 1 and 2. The sizes of the PCR products detected in YCCEL1 cells were the same as those in AGS-EBV-GFP, SNU-719 and Namalwa cells, which are infected with type 1 EBV (Fig. 1b).

Expression of EBV latent genes

Western blot analysis, immunofluorescence assay and RT-PCR were used to investigate the latency of EBV in YCCEL1 cells. EBV-negative BJAB cells and AGS cells did not show any sign of EBV latent gene expression, whereas the latency III EBV (+) lymphoblastoid cell line, SNU-1103, expressed EBNA1, EBNA2, LMP1, LMP2A and LMP2B (Fig. 2a, b). We are not sure why multiple bands were detected in some cell lines using mAb OT1X against EBNA1. Some of them may be non-specific bands or modified or degraded EBNA1. The latency III EBV (+) Burkitt's lymphoma cell line, Namalwa, also expressed

EBNA1 and EBNA2, but not LMP1 (Fig. 2a). The EBV gastric cancer cell lines AGS-EBV-GFP and SNU-719 expressed EBNA1 and LMP2A, but not EBNA2 and LMP1 (Fig. 2a, b). LMP2B was not detectable in YCCEL1 and SNU-719, unlike in AGS-EBV-GFP, which showed low-level expression of LMP2B mRNA (Fig. 2b). The expression patterns of latent genes in YCCEL1 cells were similar to those seen in the EBV-positive gastric cancer cell line SNU-719 (Fig. 2a–c). The EBV promoter used in YCCEL1 cells was identified by RT-PCR using specific primers for each of the three latent promoters of EBV. Cp or Wp transcripts were detected in the latency III cell lines Mutu III and Namalwa. In contrast, Qp transcripts were detected in YCCEL1 cells and in the EBV-positive GC cell lines AGS-EBV-GFP and SNU-719 (Fig. 2d).

Expression of EBV lytic genes

The effect of TPA on the induction of EBV lytic genes was analysed in YCCEL1 cells. B95-8 and SNU-719 were used for comparison and BJAB was used as a negative control. RT-PCR was performed for 30 cycles and the products were analysed by agarose gel electrophoresis (Fig. 3a). BZLF1 mRNA was shown at a low level in unstimulated B95-8 cells and increased dramatically following TPA treatment (Fig. 3a). BZLF1 mRNA expression was undetectable in basal state SNU-719, but was induced following TPA treatment. In YCCEL1, no (on 50% of occasions) or a very small amount of BZLF1 mRNA was detectable without stimulation. TPA treatment caused BZLF1 mRNA expression in YCCEL1, but the expression level was generally lower than that observed in SNU-719 (Fig. 3a).

Western blot results showed that the majority of the lytic proteins were not detectable in YCCEL1 cells even after TPA treatment (Fig. 3b). This contrasted with the results for SNU-719 which showed induced lytic protein expression following TPA treatment. Without TPA stimulation, immunofluorescence assay showed gp350 expression in 3% of B95-8 cells, but not in SNU-719 and YCCEL1 cells (Fig. 3c). TPA treatment increased gp350 expression in B95-8 and SNU-719 cells by 40% and 15%, respectively. Rarely (<1%), we detected gp350 expression in YCCEL1 cells.

Clonality of EBV genome and EBV copy numbers in YCCEL1 cells

To test the clonality of the EBV genome in YCCEL1, DNA extracted from YCCEL1 cells was digested with *Bam*HI and Southern blotting was carried out using a DNA probe specific for the EBV terminal repeat (TR). The TR band was not detected in the EBV-negative cell line BJAB. The TR fragments were detected at 21 kb in Raji cells and at 12 kb in SNU-719 cells, while multiple smeared bands at 8–12 kb and 4–6 kb were detected in B95-8 cells. A single

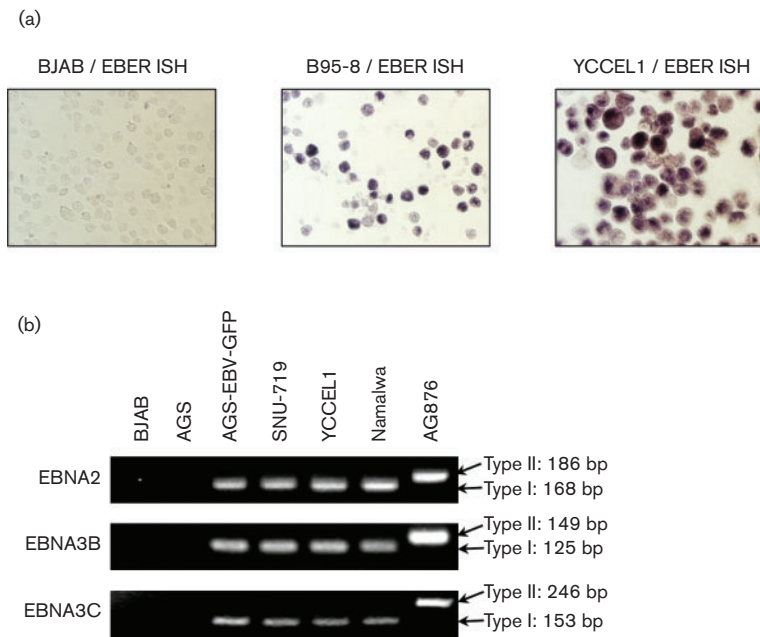


Fig. 1. Detection of EBV in YCCEL1 cells. (a) EBER *in situ* hybridization (ISH). Cells were fixed and hybridized with an EBER-specific RNA probe. Positive staining was observed under a light microscope as dark violet-blue granules at the site of hybridization (original magnification: $\times 200$). (b) Analysis of EBV type by PCR. EBNA2-, EBNA3B- and EBNA3C-specific PCR yielded products with different sizes depending on the infected EBV type. Namalwa (type I) and AG876 (type II) were used as type-specific EBV-positive controls.

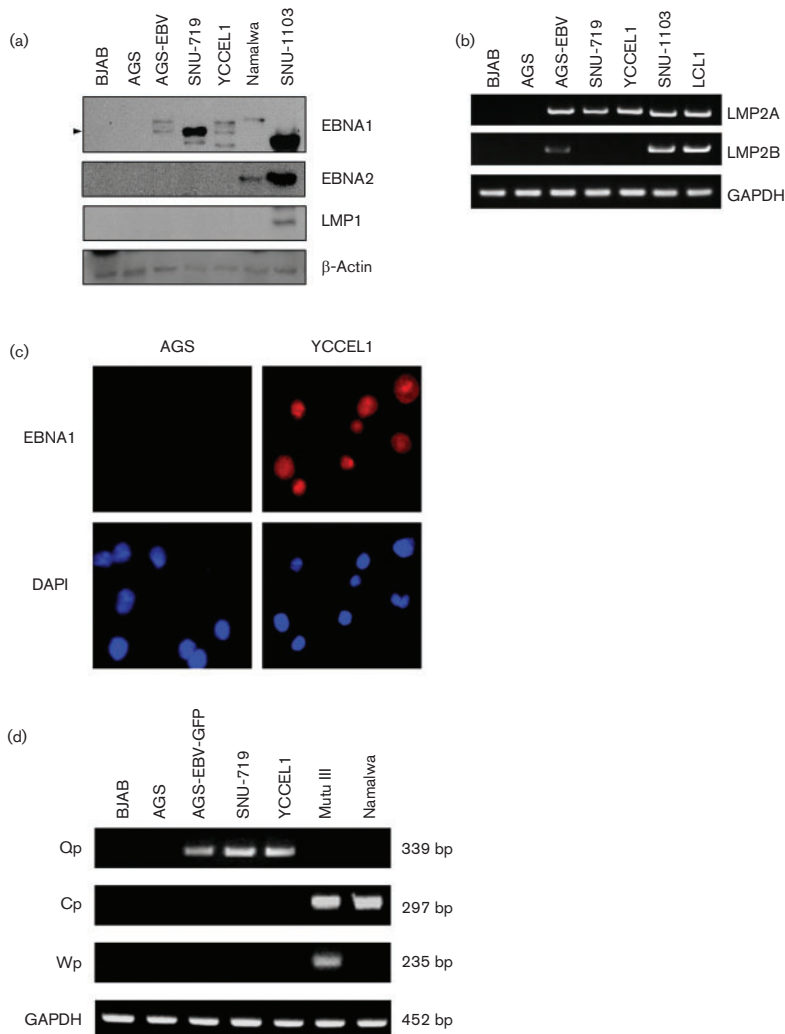


Fig. 2. EBV latent gene expression in YCCEL1 cells. (a) Detection of latent proteins. Cell lysate was prepared and 50 μg of total cellular protein from each cell line was analysed by Western blot using antibody to EBNA1, EBNA2 or LMP1. Anti- β -actin antibody (1:2000) was used to check the loading amount. (b) Detection of LMP2A and LMP2B mRNA. Total RNA was extracted from each cell line. LMP2A and LMP2B expressions were analysed by RT-PCR. GAPDH was used as a loading control. (c) Immunostaining for EBNA1 YCCEL1 cells (original magnification: $\times 200$) and EBV-negative AGS cells were included to verify specificity of EBNA1 antibody. Cells were incubated with anti-EBNA1 (OT1X) antibody. (d) Analysis of latent promoter usage. A specific 3'-primer for each transcript initiating at the Cp, Wp or Qp EBV promoter was used for cDNA synthesis. The cDNA was subjected to latent EBV promoter-specific PCR. GAPDH mRNA was amplified to compare the quantity and quality of the RNA samples.

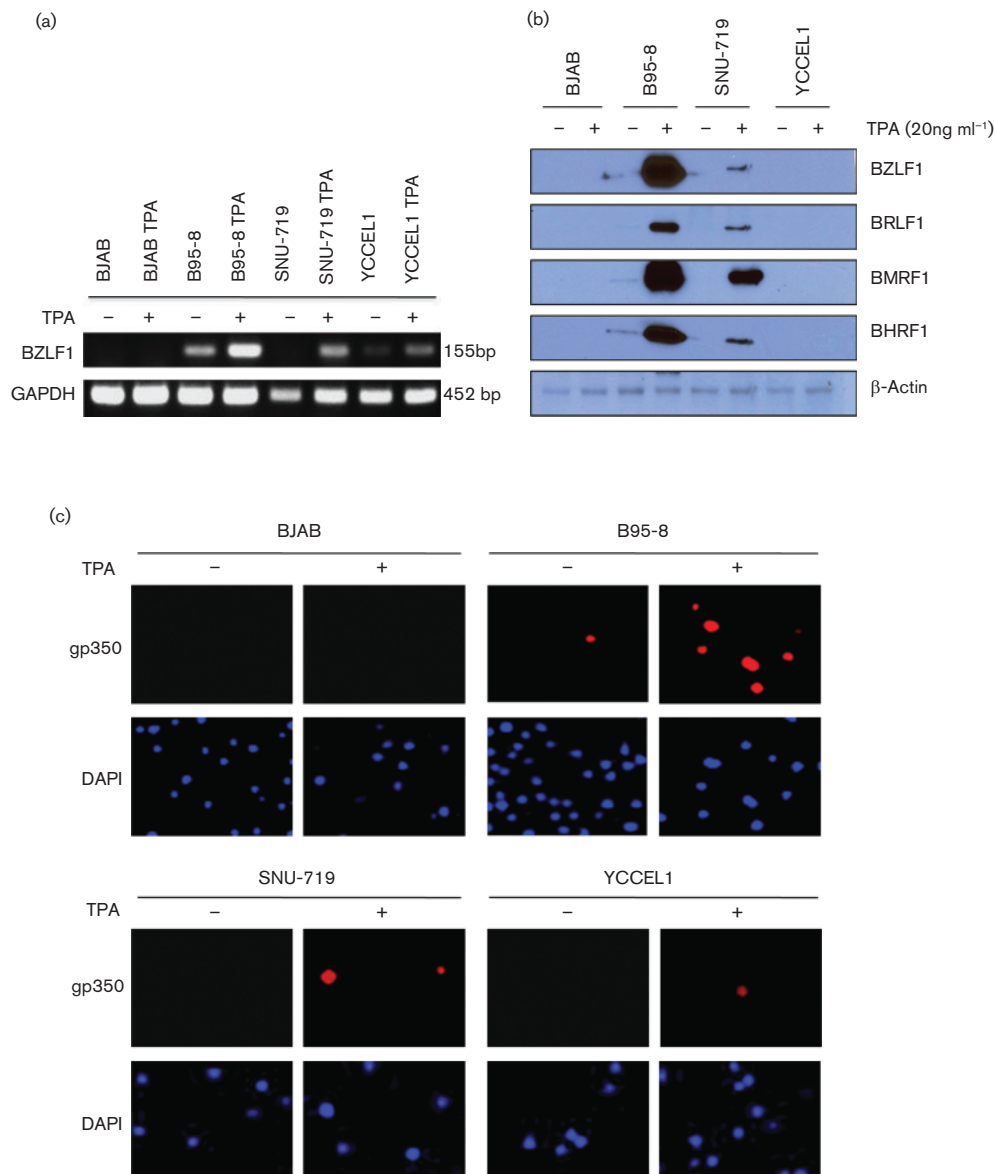


Fig. 3. EBV lytic gene expression in YCCEL1 cells. Cells were treated with TPA (20 ng ml^{-1}) for 4 days to induce the lytic cycle. (a) RT-PCR analysis of BZLF1 expression. Total cellular RNA was used to access the level of BZLF1 mRNA. EBV-negative BJAB cells served as a negative control for BZLF1 expression. GAPDH mRNA was amplified to compare the quantity and quality of the RNA samples. (b) Detection of lytic proteins. Cell lysate was prepared and $30 \mu\text{g}$ of total cellular protein from each cell line was analysed by Western blotting using antibodies to BZLF1, BRLF1, BMRF1 or BHRF1. Anti- β -actin antibody (1 : 2000) was used to check the loading amount. (c) Immunostaining for gp350 in YCCEL1 cells. Expression of gp350 was detected by incubating with anti-gp350 antibody followed by Cy3-conjugated secondary antibody. B95-8 and SNU-719 was used as a positive control for gp350 expression. BJAB was used as a negative control (original magnification: $\times 200$).

TR band was detected at 15 kb in YCCEL1 cells (Fig. 4a). Real-time PCR was carried out for EBNA1 within the EBV genome to access the EBV copy number in YCCEL1 cells. The EBV genome was not detected in BJAB cells, which were used as a negative control, while a very low level of EBV genome was detected in Namalwa cells. EBV copy number detected in YCCEL1 cells was similar to that in SNU-719 cells (Fig. 4b).

No expression of CD21 in YCCEL1 cells

Immunofluorescence assay was used to verify whether CD21, the receptor for the infection of B-cells by EBV, was expressed in YCCEL1 cells. CD19 and cytokeratin were used as markers for B-cells and epithelial cells, respectively. SNU-719, an EBV-positive gastric epithelial cell line, expressed cytokeratin, but not CD21 and CD19. BJAB, an EBV-negative B-cell line, expressed CD21 and CD19, but

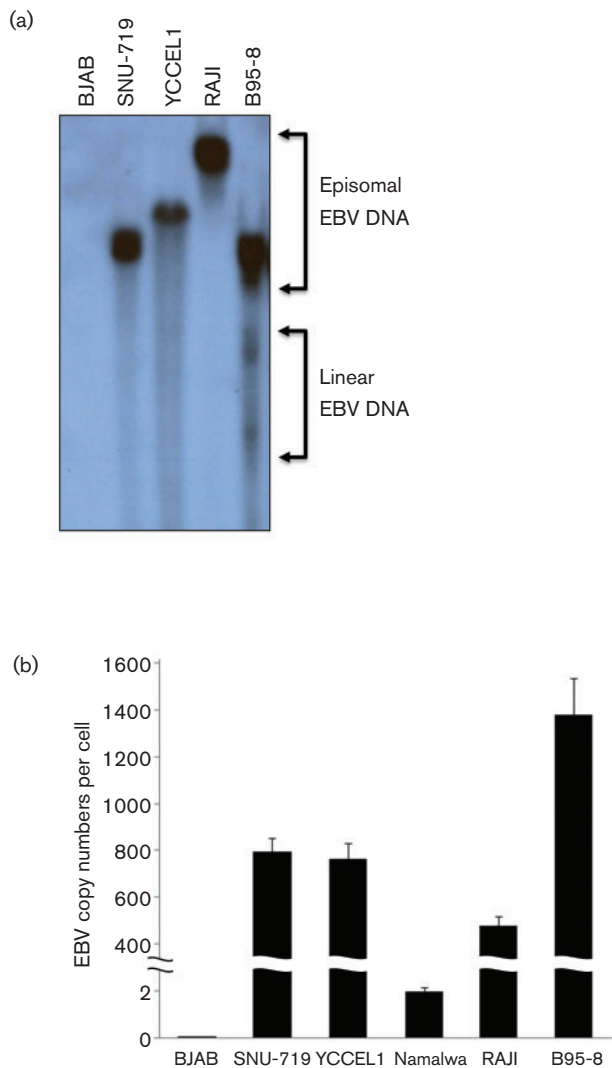


Fig. 4. Analysis of EBV genome in YCCEL1 cells. (a) Detection of the EBV TR fragment. Thirty micrograms of DNA were digested with *Bam*HI restriction enzyme, transferred to a membrane and hybridized with [α - 32 P] CTP-labelled probes. (b) Quantification of EBV DNA copies. EBV copy numbers were quantified by real-time PCR using the EBNA1 Taqman probe. BJAB was used as a negative control.

not cytokeratin. YCCEL1 cells expressed cytokeratin, but not CD21 and CD19, just like SNU-719 cells (Fig. 5).

Expression pattern of EBV miRNAs in YCCEL1 cells

The expression of EBV BHRF1 miRNAs and BART miRNAs in YCCEL1 cells was analysed by Northern blotting and qRT-PCR. YCCEL1 cells expressed higher levels of BART miRNAs than AGS-EBV-GFP, SNU-719 and SNU-1103 cells (Fig. 6a, c). The latency III cell lines Namalwa and SNU-1103 expressed BHRF1 miRNAs, while YCCEL1 cells together with the latency I cell lines AGS-EBV-GFP and

SNU-719 did not (Fig. 6a). The expression of BART transcripts in the same cell lines was also analysed by qRT-PCR (Fig. 6b). As expected, EBV-negative cell lines BJAB and AGS did not express EBV BART transcripts. In general, the expression levels of BART transcripts in EBV-positive cell lines correlated with those of BART miRNAs. However, the correlation was not very tight as the level of BART transcript was highest in SNU-719 rather than in YCCEL1 cells, which showed the highest BART miRNA expression (Fig. 6b).

DISCUSSION

The present results demonstrate the latent EBV infection of YCCEL1 cells through various analyses. EBV can be classified as types 1 or 2 according to the differences in the sequences of its EBNA2 and EBNA3 genes (Sample *et al.*, 1990). YCCEL1 cells are infected with type I EBV, similar to the majority of EBV-infected cell lines (Sample *et al.*, 1990). The latency of EBV-associated malignancies is classified into three groups according to the EBV gene expression pattern; these latency patterns are used to classify the types of EBV-associated cancers (Fukayama *et al.*, 1998). Namalwa, known as latency I/II, expresses EBNA1 and EBNA2, but not LMP1 and LMP2 (Bernasconi *et al.*, 2006; Satoh *et al.*, 2002). Also, we did not detect LMP2A expression in Namalwa cells by Western blot analysis, but did detect low levels of LMP2A mRNA by RT-PCR. The YCCEL1 cell line can be classified as showing modified latency I because it exhibits a similar pattern to the naturally EBV-infected EBVaGC cell line SNU-719 (Oh *et al.*, 2004). Conventional TPA treatment was not efficient (<1%) at inducing the lytic cycle in YCCEL1 cells, so there were too few to be detected by Western blot. The discrepancies between the protein and RNA data for BZLF1 cells may be due to a sensitivity difference between the two detection methods.

TRs of the EBV genome are the essential elements for processing and packaging EBV DNA during genome circularization (Hammerschmidt & Sugden, 1989). As established in previous studies, a single TR fragment was detected at 21 kb in Raji cells and at 12 kb in SNU-719 cells by Southern blot using a DNA probe specific for EBV TR (Oh *et al.*, 2004; Raab-Traub & Flynn, 1986). Both episomal EBV TR bands derived from latent EBV genome and linear EBV TR bands generated from the lytic EBV genome were detected in B95-8 cells (Oh *et al.*, 2004). A single TR band was detected in YCCEL1 cells, indicating that the YCCEL1 cell line is the result of clonal proliferation of a single latently EBV-infected cell. Few YCCEL1 cells undergo the lytic cycle spontaneously, judging from the fact that only one TR band was observed by Southern blotting and EBV lytic genes were not detectable in this cell line at the basal state.

Namalwa cells contain two copies of the EBV genome integrated into the cellular DNA (Andersson, 1975). In the

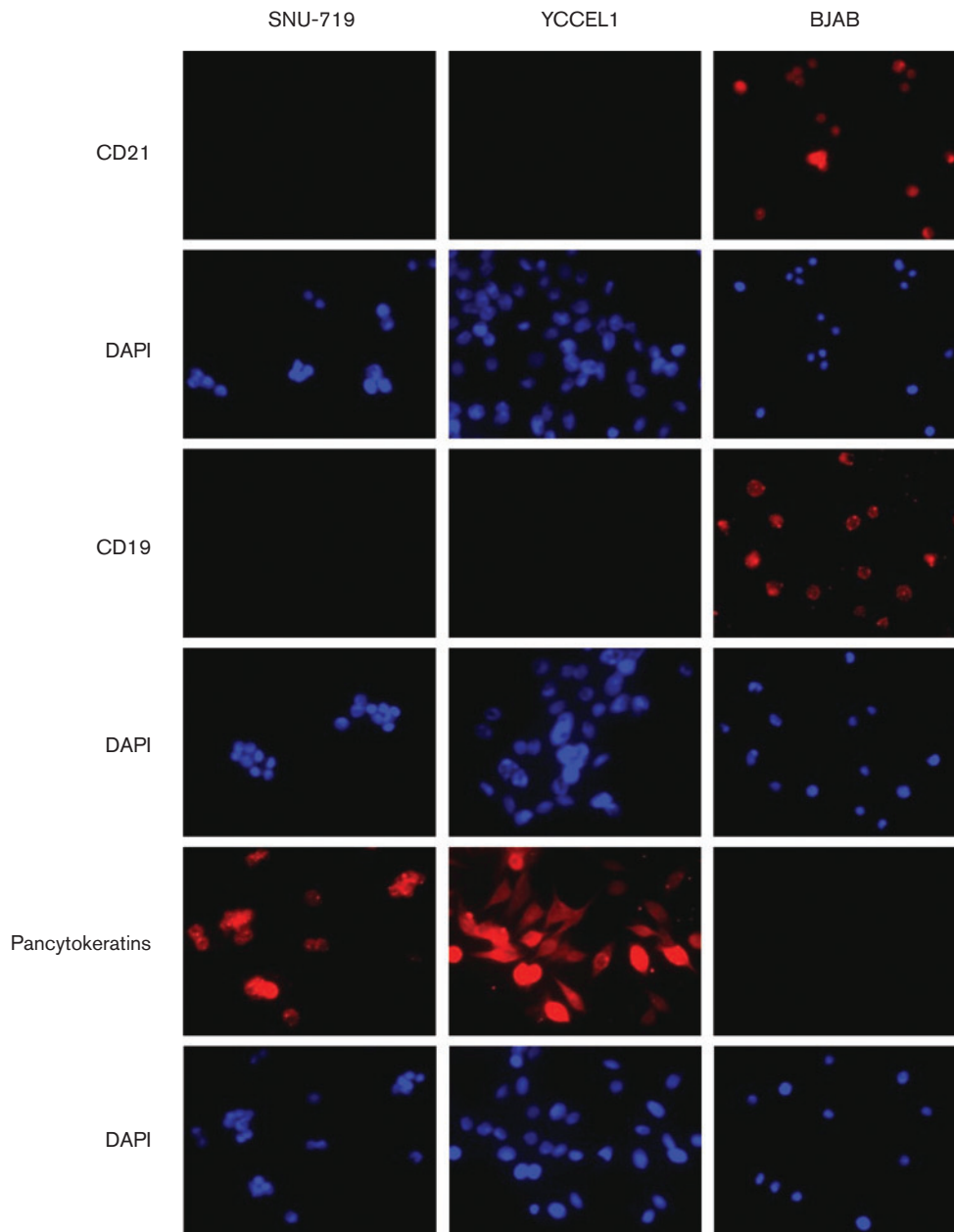


Fig. 5. Immunostaining for CD21, CD19 and cytokeratin in YCCEL1 cells. SNU-719 was used as a positive control for cytokeratin expression. BJAB was used as a positive control for CD21 and CD19 expression (original magnification: $\times 400$).

case of B95-8, a proportion of the cells are known to undergo the lytic cycle under unstimulated conditions, and this seems to be why multiple fused terminal fragments were detected in B95-8 cells (Gargouri *et al.*, 2009). The EBV copy number in YCCEL1 cells was higher than in Namalwa and Raji cells, and lower than in B95-8 cells. The EBV copy number in YCCEL1 cells was similar to that in SNU-719 cells, which is interesting in that both YCCEL1 and SNU-719 are naturally EBV-infected GC cell lines. The EBV copy number in Raji cells estimated in this study was higher than that previously reported (Klein *et al.*, 1974).

The infection of B-cells by EBV results from the direct interaction between EBV gp350/220 and cellular CD21 (Nemerow *et al.*, 1987). However, EBV also infects epithelial cells that do not express CD21. In these cases, infection seems to occur through another receptor different from CD21. Recently, it has been shown that interaction between gHgL and integrin $\alpha v \beta 6$, $\alpha v \beta 8$ and $\alpha v \beta 5$ can initiate fusion of EBV with epithelial cells (Chesnokova *et al.*, 2009). Because YCCEL1 cells do not express CD21, whereas SNU-719 cells do, these cell lines may be infected via integrins or another receptor.

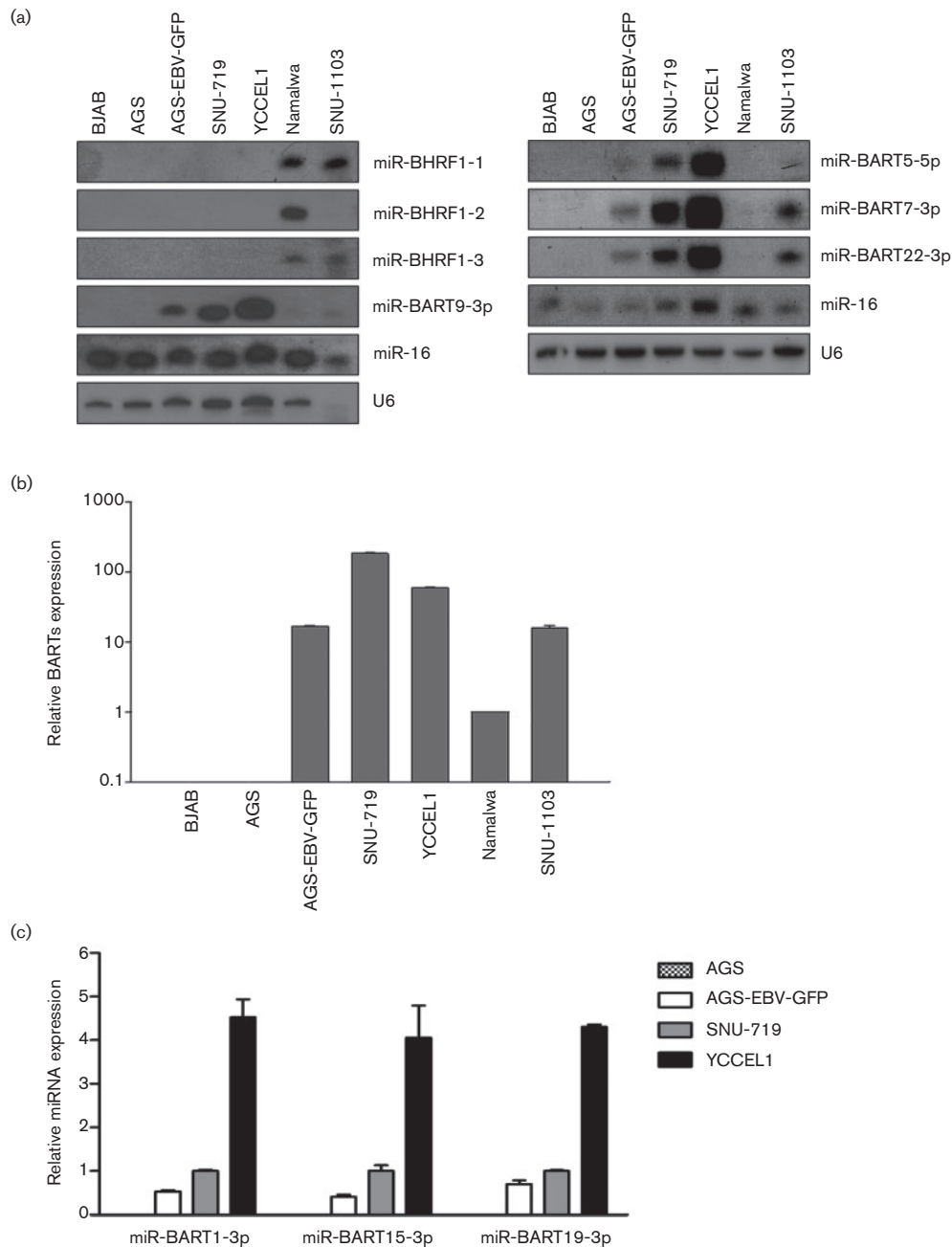


Fig. 6. Analysis of EBV miRNA expression pattern in YCCEL1 cells. (a) Northern blot analysis of EBV miRNAs; BJAB and AGS served as negative controls. AGS-EBV-GFP and SNU-719 were used as positive controls for BART miRNAs, while Namalwa and SNU-1103 were used as positive controls for BHRF1 miRNAs. The U6 snRNA was used as a loading control. The expression of the cellular miR-16 was assessed as a reference. A large proportion of the RNA from SNU-1103 cells was lost during the experiments shown on the left panel as noticeable from the miR-16 and U6 bands. (b) Analysis of EBV BART transcript expression. The expression of BART transcripts in the cells was assayed by qRT-PCR in triplicate. The expression of BART transcripts was normalized using the expression of GAPDH in each cell line; the results were then expressed relative to that in Namalwa which showed the lowest BART transcripts. BJAB and AGS served as negative controls. (c) The expression of miR-BART1-3p, 15-3p and 19-3p was assayed by qRT-PCR in triplicate. Expression of each miR-BART miRNA was first normalized using that of U6 snRNA in the same cell line; the results were then expressed relative to that in SNU-719.

YCCEL1 cells did not express BHRF1 miRNA, like AGS-EBV-GFP and SNU-719 cells. However, the expression of miR-BART1-3p, 5-5p, 7-3p, 15-3p, 19-3p and 22-3p was detected in AGS-EBV-GFP, SNU-719 and YCCEL1 cells by Northern blot and qRT-PCR. The expression pattern of EBV miRNAs in YCCEL1 cells was similar to that reported in EBV-associated GC and tissues (Kim *et al.*, 2007). BART miRNAs were expressed to a greater extent in YCCEL1 cells than in the other cell lines examined. As the expression levels of BART miRNAs correlate with that of BART transcripts in general, BART miRNAs seemed to be expressed more highly than expected in YCCEL1 cells. The reason for this disparity is unclear, but it could be due to different processing and/or stability of miRNAs in different cell lines.

Because the EBV gene expression pattern of YCCEL1 cells closely resembles that of EBVaGC cases, this naturally EBV-infected cell line may serve as a valuable model system to clarify the function of EBV in GC.

METHODS

Establishment of an EBV-infected gastric carcinoma cell line YCCEL1. The YCCEL1 cell line was established from the ascitic fluid of a pathologically proven gastric cancer patient, a 64 year-old-Korean male with advanced gastric cancer with carcinomatosis, and the biopsy showed poorly differentiated adenocarcinoma. Ascitic fluid was collected, pelleted, washed and resuspended in minimum essential medium (MEM) supplemented with 10% heat-inactivated FBS. Initially, 5×10^5 cells were seeded into 25 cm² flasks and adherent cultures were passaged whenever vigorous tumour cell growth was observed. Subsequent passages were performed weekly after trypsinization at subconfluence. During the initial culture, differential trypsinization was used to obtain a pure tumour cell population when stromal cell growth was noted.

Cell culture. EBV-positive cell lines (AGS-EBV-GFP, SNU-719, Mutu III, Namalwa, SNU-1103, B95-8, LCL1 and Raji) and EBV-negative cell lines (BJAB and AGS) were used. The cells were maintained in RPMI 1640 (Gibco-BRL) supplemented with 10% FBS and maintained at 37 °C in a 5% CO₂ incubator.

RNA and genomic DNA extraction. RNA extraction was conducted with RNazol B reagent (Tel-Test) according to the manufacturer's instructions. DNA was extracted from the cells by the standard phenol/chloroform technique. Briefly, for cell lysis, EBV-infected cell lines were incubated for 15 h at 55 °C with TE buffer (pH 8.0) containing proteinase K (200 µg ml⁻¹) and 0.5% SDS. Genomic DNA was obtained using phenol/chloroform extraction, and the aqueous fraction was collected. Genomic DNA was precipitated with 2-propanol and washed with 70% ethanol. The DNA was dried at room temperature and dissolved in distilled water.

RT-PCR and DNA PCR. First-strand cDNA synthesis was performed using 1 µg total RNA and a 3'-primer specific for each transcript initiating at the Cp, Wp or Qp EBV promoter. The cDNA samples were then subjected to PCR using appropriate primer pairs for the transcripts initiating at the Cp, Wp or Qp (Sugiura *et al.*, 1996). Each cycle consisted of denaturation for 30 s at 94 °C, annealing for 30 s at 59 °C and extension for 30 s at 72 °C. The PCR products were electrophoresed in a 1.5% agarose gel (Kim *et al.*, 2011). Distinguishing between EBV types 1 and 2 was accomplished using specific PCR primers for EBNA2, EBNA3B and EBNA3C (Oh *et al.*,

2004). The PCR primer sequences used for LMP2A and LMP2B RT-PCR were as reported previously (Oh *et al.*, 2004).

In situ hybridization for EBV encoded RNAs. *In situ* hybridization was performed using the ZytoFast EBV-CISH system (ZytoVision), which is designed for the detection of EBERs. The EBER oligonucleotide probe is directed against EBER-1 and EBER-2 RNA sequences transcribed in latently EBV-infected cells. Slides were fixed, predigested by pepsin diluents (5 min, 37 °C) and hybridized with the EBER oligonucleotide probe tagged with Biotin (1 h, 55 °C). Alkaline phosphatase-conjugated-streptavidin was then applied for detection (30 min, 37 °C). Nitro blue tetrazolium chloride/5-bromo-4-chlor-3-indolyl phosphate, toluidine salt (NBT/BCIP) was used as chromogen (20–40 min, 37 °C). All slides were kept in a moisture chamber during the procedures.

Western blot analysis. To detect the expression of EBV lytic genes in various cell lines, anti-BZLF1 (Dako; 1:500), anti-BRLF1 (Argene; 1:500), anti-BMRF1 (Novocastra; 1:500) and anti-BHRF1 (3E8, 1:250) (Chou *et al.*, 2004) antibodies were used. To detect the expression of EBV latent genes, anti-EBNA1 (gift from Dr Jaap Middeldorp, VU University Medical Center, The Netherlands; 1:1000), anti-EBNA2 (Dako; 1:500) and anti-LMP1 (Dako; 1:500) antibodies were used. Anti-β-actin (Cell Signalling Technologies; 1:2000) antibody was also used to confirm comparable loading.

Immunofluorescence assay. Cells were harvested and attached to 12-well multi-test slides. After the cells had been fixed with 4% paraformaldehyde, they were blocked with 20% normal goat serum. The cells were incubated with anti-EBNA1 (1:100) antibodies. Following incubation with Cy3-labelled secondary antibody, the slides were treated with 4',6-diamidino-2-phenylindole (DAPI) mounting solution (Invitrogen). Protein expression was observed using an Axiovert 200 fluorescence microscope (Carl Zeiss).

To detect expression of EBV lytic genes, cells were treated with 20 ng ml⁻¹ of 12-O-tetradecanoylphorbol-13-acetate (TPA) for 4 days before experiments. The cells were harvested and attached to 12-well multi-test slides. To detect expression of CD21, CD19 and cytokeratins, cells were cultured in eight-well chamber slides. Cells were fixed with 100% ice-cold acetone. After blocking with 20% normal goat serum, cells were incubated with anti-gp350 (Chemicon; 1:200), anti-CD21 (Abcam; 1:200), PE-conjugated anti-CD19 (BioLegend; 1:100) and anti-pancytokeratin (Invitrogen; 1:200) antibodies. Following incubation with Cy3-labelled secondary antibody, slides were treated with DAPI-mounting solution (Invitrogen). Protein expression was observed using an Axiovert 200 fluorescence Microscope (Carl Zeiss).

Southern blot analysis. Purified genomic DNA (30 µg) was digested for 15 h with *Bam*HI. The digested DNA was separated on a 0.7% agarose gel and denatured for 30 min in 0.25 N HCl. The DNA was transferred to a Hybond-N⁺ membrane (Amersham). The membrane was pre-hybridized using ExpressHyb Hybridization Solution (Clontech) with salmon sperm DNA and hybridized at 60 °C for 1 h with a ³²P-labelled specific probe for EBV terminal repeat sequence. After washing using wash solution containing 2 × standard saline citrate and 1% SDS, the membrane was exposed to X-ray film at -70 °C for 4 h.

Quantitative PCR to access EBV genome copies. Genomic DNA was used for Q-PCR assay to determine the EBV-DNA copy number per cell. Q-PCR was performed using 200 ng genomic DNA. Sequences of the EBNA1 primer and Taqman probe used for Q-PCR were as follows: primer 5'-GGATGCGATTAAGGACCTTGTT-3' and 5'-AAAGCTGCACACAGTCACCT-3', probe 5'-FAM-TG-ACAAAGCCCCTCTACTCTGCAAT-TAMSp-3'. The thermocycling conditions were 45 cycles of 95 °C for 5 s and 55 °C for 25 s

with an initial cycle of 95 °C for 30 s. Specific product was detected using the MX-3000P (Stratagene) detector for quantification. EBV copy numbers were calculated based on the facts that Namalwa cells have two copies of the EBV genome per cell (Andersson, 1975).

Small RNA extraction and Northern blot analysis. Small RNA was extracted using a mirVana microRNA Isolation kit (Ambion) according to the manufacturer's protocol. For the Northern blot analysis of EBV miRNA expression, 1 µg small RNA per sample was electrophoresed in 15% polyacrylamide-urea gel and transferred onto a Zeta-Probe blotting membrane (Bio-Rad Laboratories). Oligonucleotides complementary to each mature EBV miRNA were end-labelled with [γ -³²P] ATP as a probe (Kim *et al.*, 2011). Hybridization was performed in ExpressHyb hybridization solution (Clontech).

Real-time qPCR for BART transcripts. Total cellular RNA was reverse-transcribed with random hexamers using the MMLV-RT system (Invitrogen). The gene-specific primers used were BART 5'-ATGCTGCTGGTGTGCTGTAA-3' and 5'-GCGGTGCTATGGACCTGTAT-3', GAPDH 5'-CATGAGAAGTATGACAACAGCCT-3' and 5'-AGTCCTTCCACGATACCAAAGT-3'. Quantitative real-time RT-PCR of BART and GAPDH was carried out on an MX-3000p Real-Time PCR machine (Agilent Life Sciences) using SYBR Premix Ex Taq (Tli RNaseH Plus) (Takara Bio).

Real-time qPCR for BART miRNAs. TaqMan microRNA assay (Applied Biosystems) was used to quantify the relative expression levels of miR-BART1-3p, miR-BART15-3p, miR-BART19-3p and U6 snRNA, which was used as an internal control. cDNA was synthesized using a TaqMan microRNA reverse transcription kit. Briefly, for each 7 µl reverse transcription (RT) master mixture, we combined 0.15 µl 100 mM dNTPs, 1 µl MultiScribe reverse transcriptase, 1.5 µl 10 × RT buffer, 0.19 µl RNase inhibitor and 4.16 µl nuclease-free water. The 7 µl RT master mixture was then combined in a fresh tube with 5 µl total RNA (1 ng) and 3 µl RT primer (specific to each TaqMan assay), and gently mixed. The RT reactions were then performed on a DNA Engine thermal cycler (Bio-Rad) programmed to incubate the reactions at 16 °C for 30 min, 42 °C for 30 min and 85 °C for 5 min. TaqMan qRT-PCRs were carried out a Mx3000P real-time PCR system (Stratagene). Each qRT-PCR was performed in 20 µl volume, containing 10 µl TaqMan universal PCR master mix II, 1 µl 20 × TaqMan microRNA assay mix, 8 µl RNase-free water and 1 µl single-stranded cDNA product. Experiments were carried out in triplicate for each sample. Relative gene expression was calculated according to the comparative C_t method using U6 snRNA as an internal standard.

ACKNOWLEDGEMENTS

This work was supported by grants from the National Research Foundation of Korea (NRF) funded by the Korean government (MEST) (No. 5-2011-A0154-00072) and the Gyeonggi Regional Research Centre (GRRC) of the Catholic University of Korea [(GRRC Catholic, 2012-B05), RNA-based development of biopharmaceutical lead molecules]. Dr S. Y. Rha's research was supported by the Public Welfare & Safety Research Program through the National Research Foundation of Korea (NRF) funded by the Ministry of Education, Science and Technology (2010-0020841). We thank Hyoung June Kwon for helping with the manuscript preparation.

REFERENCES

Andersson, M. (1975). Amounts of Epstein-Barr virus DNA in somatic cell hybrids between Burkitt lymphoma-derived cell lines. *J Virol* **16**, 1345–1347.

Bernasconi, M., Berger, C., Sigrist, J. A., Bonanomi, A., Sobek, J., Niggli, F. K. & Nadal, D. (2006). Quantitative profiling of housekeeping and Epstein-Barr virus gene transcription in Burkitt lymphoma cell lines using an oligonucleotide microarray. *Virology* **3**, 43.

Chesnokova, L. S., Nishimura, S. L. & Hutt-Fletcher, L. M. (2009). Fusion of epithelial cells by Epstein-Barr virus proteins is triggered by binding of viral glycoproteins gHgL to integrins $\alpha v\beta 6$ or $\alpha v\beta 8$. *Proc Natl Acad Sci U S A* **106**, 20464–20469.

Chou, S. P., Tsai, C. H., Li, L. Y., Liu, M. Y. & Chen, J. Y. (2004). Characterization of monoclonal antibody to the Epstein-Barr virus BHRF1 protein, a homologue of Bcl-2. *Hybrid Hybridomics* **23**, 29–37.

Danve, C., Decaussin, G., Busson, P. & Ooka, T. (2001). Growth transformation of primary epithelial cells with a NPC-derived Epstein-Barr virus strain. *Virology* **288**, 223–235.

Fukayama, M., Chong, J. M. & Kaizaki, Y. (1998). Epstein-Barr virus and gastric carcinoma. *Gastric Cancer* **1**, 104–114.

Gargouri, B., Van Pelt, J., El Feki, A. F., Attia, H. & Lassoued, S. (2009). Induction of Epstein-Barr virus (EBV) lytic cycle in vitro causes oxidative stress in lymphoblastoid B cell lines. *Mol Cell Biochem* **324**, 55–63.

Hammerschmidt, W. & Sugden, B. (1989). Genetic analysis of immortalizing functions of Epstein-Barr virus in human B lymphocytes. *Nature* **340**, 393–397.

Iwasaki, Y., Chong, J. M., Hayashi, Y., Ikeno, R., Arai, K., Kitamura, M., Koike, M., Hirai, K. & Fukayama, M. (1998). Establishment and characterization of a human Epstein-Barr virus-associated gastric carcinoma in SCID mice. *J Virol* **72**, 8321–8326.

Kim, N., Chae, H. S., Oh, S. T., Kang, J. H., Park, C. H., Park, W. S., Takada, K., Lee, J. M., Lee, W. K. & Lee, S. K. (2007). Expression of viral microRNAs in Epstein-Barr virus-associated gastric carcinoma. *J Virol* **81**, 1033–1036.

Kim, N., Song, Y. J. & Lee, S. K. (2011). The role of promoter methylation in Epstein-Barr virus (EBV) microRNA expression in EBV-infected B cell lines. *Exp Mol Med* **43**, 401–410.

Klein, G., Lindahl, T., Jondal, M., Leibold, W., Menézes, J., Nilsson, K. & Sundström, C. (1974). Continuous lymphoid cell lines with characteristics of B cells (bone-marrow-derived), lacking the Epstein-Barr virus genome and derived from three human lymphomas. *Proc Natl Acad Sci U S A* **71**, 3283–3286.

Middeldorp, J. M., Brink, A. A., van den Brule, A. J. & Meijer, C. J. (2003). Pathogenic roles for Epstein-Barr virus (EBV) gene products in EBV-associated proliferative disorders. *Crit Rev Oncol Hematol* **45**, 1–36.

Miller, G. & Lipman, M. (1973). Release of infectious Epstein-Barr virus by transformed marmoset leukocytes. *Proc Natl Acad Sci U S A* **70**, 190–194.

Miller, G., Enders, J. F., Lisco, H. & Kohn, H. I. (1969). Establishment of lines from normal human blood leukocytes by co-cultivation with a leukocyte line derived from a leukemic child. *Proc Soc Exp Biol Med* **132**, 247–252.

Nemerow, G. R., Mold, C., Schwend, V. K., Tollefson, V. & Cooper, N. R. (1987). Identification of gp350 as the viral glycoprotein mediating attachment of Epstein-Barr virus (EBV) to the EBV/C3d receptor of B cells: sequence homology of gp350 and C3 complement fragment C3d. *J Virol* **61**, 1416–1420.

Oh, S. T., Seo, J. S., Moon, U. Y., Kang, K. H., Shin, D. J., Yoon, S. K., Kim, W. H., Park, J. G. & Lee, S. K. (2004). A naturally derived gastric cancer cell line shows latency I Epstein-Barr virus infection closely resembling EBV-associated gastric cancer. *Virology* **320**, 330–336.

Park, J. G., Yang, H. K., Kim, W. H., Chung, J. K., Kang, M. S., Lee, J. H., Oh, J. H., Park, H. S., Yeo, K. S. & other authors (1997).

Establishment and characterization of human gastric carcinoma cell lines. *Int J Cancer* **70**, 443–449.

Raab-Traub, N. & Flynn, K. (1986). The structure of the termini of the Epstein-Barr virus as a marker of clonal cellular proliferation. *Cell* **47**, 883–889.

Sample, J., Young, L., Martin, B., Chatman, T., Kieff, E., Rickinson, A. & Kieff, E. (1990). Epstein-Barr virus types 1 and 2 differ in their EBNA-3A, EBNA-3B, and EBNA-3C genes. *J Virol* **64**, 4084–4092.

Satoh, T., Fukuda, M. & Sairenji, T. (2002). Distinct patterns of mitogen-activated protein kinase phosphorylation and Epstein-Barr virus gene expression in Burkitt's lymphoma cell lines versus B lymphoblastoid cell lines. *Virus Genes* **25**, 15–21.

Shannon-Lowe, C. D., Neuhierl, B., Baldwin, G., Rickinson, A. B. & Delecluse, H. J. (2006). Resting B cells as a transfer vehicle for Epstein-Barr virus infection of epithelial cells. *Proc Natl Acad Sci U S A* **103**, 7065–7070.

Shimizu, N., Yoshiyama, H. & Takada, K. (1996). Clonal propagation of Epstein-Barr virus (EBV) recombinants in EBV-negative Akata cells. *J Virol* **70**, 7260–7263.

Sugiura, M., Imai, S., Tokunaga, M., Koizumi, S., Uchizawa, M., Okamoto, K. & Osato, T. (1996). Transcriptional analysis of Epstein-Barr virus gene expression in EBV-positive gastric carcinoma: unique viral latency in the tumour cells. *Br J Cancer* **74**, 625–631.

Tajima, M., Komuro, M. & Okinaga, K. (1998). Establishment of Epstein-Barr virus-positive human gastric epithelial cell lines. *Jpn J Cancer Res* **89**, 262–268.

Takada, K. (2000). Epstein-Barr virus and gastric carcinoma. *Mol Pathol* **53**, 255–261.

Takasaka, N., Tajima, M., Okinaga, K., Satoh, Y., Hoshikawa, Y., Katsumoto, T., Kurata, T. & Sairenji, T. (1998). Productive infection of Epstein-Barr virus (EBV) in EBV-genome-positive epithelial cell lines (GT38 and GT39) derived from gastric tissues. *Virology* **247**, 152–159.

Teramoto, N., Maeda, A., Kobayashi, K., Hayashi, K., Oka, T., Takahashi, K., Takada, K., Klein, G. & Akagi, T. (2000). Epstein-Barr virus infection to Epstein-Barr virus-negative nasopharyngeal carcinoma cell line TW03 enhances its tumorigenicity. *Lab Invest* **80**, 303–312.

Yoshiyama, H., Shimizu, N. & Takada, K. (1995). Persistent Epstein-Barr virus infection in a human T-cell line: unique program of latent virus expression. *EMBO J* **14**, 3706–3711.

Yoshiyama, H., Imai, S., Shimizu, N. & Takada, K. (1997). Epstein-Barr virus infection of human gastric carcinoma cells: implication of the existence of a new virus receptor different from CD21. *J Virol* **71**, 5688–5691.

Young, L. S. & Rickinson, A. B. (2004). Epstein-Barr virus: 40 years on. *Nat Rev Cancer* **4**, 757–768.